



Published in final edited form as:

J Mol Biol. 2008 March 28; 377(3): 774–789. doi:10.1016/j.jmb.2007.12.077.

Genomic and Proteomic Analysis of phiEco32, a Novel *Escherichia coli* Phage

Dhruvi Savalia^{1,#}, Lars F. Westblade^{2,#}, Manisha Goel³, Laurence Florens³, Priscilla Kemp⁴, Natalja Akulenko⁵, Olga Pavlova⁵, Julio C. Padovan⁶, Brian T. Chait⁶, Michael P. Washburn³, Hans-W. Ackermann⁷, Arcady Mushegian^{3,8}, Tarasii Gabisonia⁹, Ian Molineux^{4*}, and Konstantin Severinov^{1,5,10*}

¹Waksman Institute for Microbiology, Piscataway, NJ 08854

²Rockefeller University, New York, NY 10021

³Stowers Institute for Medical Research, Kansas City, MO 64110

⁴Molecular Genetics and Microbiology, and Institute for Cell and Molecular Biology, University of Texas, Austin TX 78712

⁵Institute of Molecular Genetics, Moscow 123182, Russia

⁶Laboratory for Mass Spectrometry and Gaseous Ion Chemistry, Rockefeller University, New York, NY 10065

⁷Félix d'Herelle Reference Center for Bacterial Viruses, Faculty of Medicine, Laval University, Quebec, Qc, Canada

⁸Department of Microbiology, Kansas University Medical Center, Kansas City KS 66160

⁹Eliava Bacteriophage Institute, Tbilisi, Republic of Georgia

¹⁰Institute of Gene Biology, Moscow 117312, Russia,

SUMMARY

A novel phage infecting *Escherichia coli* was isolated during a large-scale screen for phages that may be used for therapy of mastitis in cattle. The 77,554 bp genome of the phage, named phiEco32, was sequenced and annotated, and its virions were characterized by electron microscopy and proteomics. Two phiEco32-encoded proteins that interact with host RNA polymerase were identified. One of them is an ECF-family σ -factor that may be responsible for transcription of some viral genes. Another RNA polymerase-binding protein is a novel transcription inhibitor whose mechanism of action remains to be defined.

Keywords

bacteriophage; *Podoviridae*; *E. coli*; genome; MudPIT; RNA polymerase-binding proteins

*Corresponding authors: Molecular Genetics and Microbiology, University of Texas, Austin TX 78712, Phone: (512) 471-3143; FAX (512) 471-7088; E-mail: molineux@mail.utexas.edu, Waksman Institute for Microbiology, 190 Frelinghuysen Road, Piscataway, NJ, 08854, Phone: (732) 445-6095; FAX: (732) 445-5735; E-mail: severik@waksman.rutgers.edu.

#These authors contributed equally to this work

Publisher's Disclaimer: This is a PDF file of an unedited manuscript that has been accepted for publication. As a service to our customers we are providing this early version of the manuscript. The manuscript will undergo copyediting, typesetting, and review of the resulting proof before it is published in its final citable form. Please note that during the production process errors may be discovered which could affect the content, and all legal disclaimers that apply to the journal pertain.

INTRODUCTION

Bacteriophages (phages) are the most abundant and diverse form of life on Earth and exert a major influence over the microbial world.^{1,2} To date, more than 400 phage genomes have been completely sequenced (NCBI, National Center for Biotechnology Information – July 2007). Comparative analysis has provided important insights into diversity and evolution of phage genomes and the functions of various phage genes.^{3,4} The actual number of different phages on the planet has been estimated at $\sim 10^{31}$.⁵ Nevertheless, for a given host, the number of different phages (defined here as phages that rely on different, non-homologous mechanisms of genome replication, host shut-off, and viral gene expression strategies) appears to be finite. For example, finding a truly new phage for *Escherichia coli* (*E. coli*) is quite rare and most new isolates are simple variations of known phages with identical sets of genes and more than 90% identity at the DNA level. Therefore, most phages infecting *E. coli* must have already been isolated during the many years of study of this model bacterium. In contrast, the genomic analysis of mycobacterial and *Thermus* phages continues to reveal novel genomes^{5,6}, reflecting that our knowledge of phages infecting these less studied hosts is at its infancy. On the other hand, the comparative analysis of phages infecting different hosts indicates that *i*) there is a significant genetic exchange between phages and *ii*) similar mechanisms (for example, factor-dependent antitermination of transcription of long operons containing the structural proteins of many siphoviruses such as phage λ ⁷) are often used to regulate coordinate expression of viral genes. However, phage regulators that perform apparently similar regulatory functions are often non-homologous.⁸ Identification and comparative mechanistic analysis of such regulators can be instructive as it reveals how common regulatory responses of bacterial RNA polymerase, an essential cellular molecular machine, are elicited by interactions with very different proteins.

We are engaged in a program of isolating phages infecting *E. coli* and determining the mechanisms of gene expression control that these phages use. To this end, a large collection of phages from the Eliava Institute, Tbilisi, Republic of Georgia, was surveyed for the presence of previously unreported phages. We hypothesized that the relative isolation of the Institute may help identify new phages. Here we report the identification of one such phage, *E. coli* phage phiEco32, and its genomic and proteomic analyses.

RESULTS

Isolation of phiEco32 and virion morphology

PhiEco32 was isolated in 2004 from the Kura river in Tbilisi, Georgia. It was later found to lyse 95% of *E. coli* strains isolated from cows suffering from acute mastitis and is a component of a polyvalent phage preparation currently being tested in experimental mastitis phage therapy trials (TG, KS, IJM, to be published). Its latent period at 37°C in rich media is 30 – 35 min. Virions of phiEco32 (Fig. 1) belong to the family *Podoviridae* and have a C3 morphotype⁹. The dimensions of phiEco32 are $\sim 145 \times 44$ nm for the head and $\sim 13 \times 8$ nm for the tail, with short, possibly kinked tail fibers folded on the tail.

Overview of the phiEco32 genome

The genome of phage phiEco32 consists of 77,554 bases pairs with a G+C content of 42.27%, which is significantly lower than the G+C content of the *E. coli* host (50–51%). The initial sequence of the phiEco32 genome assembled as a circle. However, restriction enzyme digests suggested both that the genome was linear and lacked cohesive ends, and also that there was ~ 200 bp of additional sequence not present in the assembled genome. The sequence of the right end of the genome (corresponding to bp 77,362–77,554) was determined by primer walking using phiEco32 genomic DNA as template. The exact left end could not be accurately

determined by this procedure as no abrupt drop-off in the intensity of peaks on the electrophoregram was reproducibly observed. A *SalI* fragment that corresponded to the left genome end was therefore isolated, ligated to *HincII*-cut pUC19 and subjected to sequencing using a plasmid-specific primer. The first non-plasmid base determined by this procedure corresponds to bp 1 of the phiEco32 genome. A similar procedure at the right genome end confirmed that bp 77,554 is the terminal nucleotide. The results of this analysis reveal a 193-bp direct repeat that defines the genome ends. Neither repeat is predicted to be part of a coding sequence. The replication strategy of phiEco32 may thus be similar to that of the T7 phage group, with formation of either circular or linear concatemeric DNA during infection to allow duplication of genome ends. The observation that the right genome end sequence of the phiEco32 genome is constant while a minor fraction of the left end is heterogeneous suggests that the initial cleavage by phiEco32 terminase may release the mature right end. The mature left end must then be a product of duplication of the next terminal repeat in a concatemeric molecule or, as apparently occurs in a few packaged genomes, be created by a less-specific cleavage in the next genome of the concatemer. Preparations of deletion mutants, in particular, of T7 also show some heterogeneity at their left genome ends (IJM, unpublished observation). The close similarity of the large terminase subunit (ORF7, Table 1) to their P22 family counterparts is consistent with the blunt ends of the phiEco32 genome and perhaps with the heterogeneity seen at the left genome end (P22-like phages package by a headful mechanism). However, it is not consistent with the T7-like sequence-specific cleavage and direct repeats at the phiEco32 genome ends. Terminases that generate the direct repeats characteristic of the T7 phage family fall into a cluster distinct from the P22-like headful enzymes.¹⁰ However, both phiEco32 ORF7 and the P22 terminase family are also closely related in sequence to the PaP3 terminase, which has been described as generating 5' protruding cohesive ends.¹¹ Terminases that generate the latter type of genome ends also usually cluster in a group distinct from the P22 family¹⁰, perhaps suggesting that both the phiEco32 and PaP3 enzymes have only recently acquired sequence-specific cleavage activity.

A total of 128 ORFs could be predicted in the phiEco32 genome (Table 1, Fig. 2). Intergenic regions longer than 100 bases were scanned for additional genes by searching for similar sequences in Genbank and the database of unfinished microbial genomes at NCBI, but no additional ORFs were found. There are 51 cases of overlaps (from 1 to 65 bases long) between neighboring ORFs. The longest non-coding region (1,944 bases) lies between ORFs 124 and 125. The predicted ORFs encode putative proteins from 35 amino acids (ORF27 and ORF41) to 1,473 amino acids (ORF26), and more than 40% have sequence homologs in the databases (see below). Only ~70% of ORFs are preceded by recognizable Shine-Dalgarno sequences. About 15% of ORFs, in particular those that are short, have neither homologs in the databases nor well-defined Shine-Dalgarno sequences, and it remains to be seen whether they represent functional genes.

Most phiEco32 ORFs start with the AUG codon, 13 ORFs use GUG, two ORFs start with UUG, and ORF83 is predicted to use AUU. Only two *E. coli* genes: *infC*¹² and *pcnB*¹³ are known to use this codon for initiation; its predicted use in phiEco32 ORF83 is based on sequence alignments from the initiating Met through residue ~200 with phage PA11 ORF4, phage PaP3 ORF45, and various amidotransferases, including their conserved catalytic residues. UAA is the most common phiEco32 stop codon (82 ORFs), with 32 and 14 ORFs ending with, respectively, UGA and UAG. About one-fifth of phiEco32 genes (26 ORFs) are transcribed in one direction (designated as rightward in the genome map, Fig. 2) and the rest are transcribed leftward. Genes transcribed in the same direction are clustered, forming two regions of genes with similar orientations. There is no difference in average G+C content between the rightward- and leftward-transcribed regions.

Using Genskew (<http://mips.gsf.de/services/analysis/genskew>) a cumulative GC-skew plot follows the direction of transcription precisely. The maximum skew value is at bp 30,493, 11 bp after the end of the last rightward ORF, ORF26 and 166 bp downstream of the last leftward ORF, ORF27. An imperfect hairpin with a GAAA tetraloop is predicted for bps 30,490–30,517 that plausibly could serve as a bidirectional terminator of transcription. The minimum value of the cumulative GC-skew is at bp 77,232, in a noncoding region between the terminal repeat and ORF128. The corresponding maxima and minima for an AT-skew analysis are 30,570 and 74,460. Minima of both skews are often associated with origins and/or termini of bidirectional DNA replication (for a review, see Ref. 14), but this remains to be established for phiEco32. However, an origin near the left genome end would give the favorable result that transcription and replication on the phiEco32 genome are co-directional.

Using the tRNA scan-SE program, we identified one tRNA gene in the phiEco32 genome. The gene lies in the intergenic region between ORF106 and ORF107 (Fig. 2). The phiEco32 tRNA gene has a TCT anticodon and should recognize the arginine codon AGA. This codon is one of the rarest in the *E. coli* genome but is overrepresented in phiEco32 compared to the host, with a frequency (defined as in the EMBOSS package, i.e., the observed or extrapolated number of a corresponding codon per 1000 codons) of 10 in the phage but only 2 in *E. coli*. Thus, as is the case with other phages^{6,15}, phiEco32-encoded tRNA may allow efficient translation of phage mRNA in the absence of sufficient amounts of corresponding cellular tRNA. However, the phage-coded tRNA may play a more subtle role as neither the major capsid nor scaffolding proteins genes, which are among those expected to be expressed at the highest levels during infection, contain the AGA codon.

Sequence analysis of predicted phiEco32 proteins

All predicted phiEco32 proteins were compared to proteins in sequence databases using PSI-BLAST, and to databases of unfinished genomes and environmental samples using TBLASTN. The results show that about 43% of phiEco32 proteins display sequence similarity to known proteins, and most of them match proteins with known molecular functions (Table 1).

PhiEco32 proteins involved in DNA replication and recombination—PhiEco32 codes for an assortment of replication and recombination factors, including a 5'-3' exonuclease (gp33), DNA polymerase (gp53), 3'-5' exonuclease (gp74), primase/helicase (gp75), and NAD-dependent DNA ligase (gp62). Gp53 is a member of DNA polymerase Family A (pfam00476) which shares significant similarity with the polymerase domain of *E. coli* DNA polymerase I. In most known Family A DNA polymerases, this domain is fused to one or two exonuclease domains, whereas the phiEco32 arrangement, where both exonucleases are represented by separate noncontiguous genes, was heretofore observed only once, in *Pseudomonas* phage PaP3. Finally, gp67, which is a member of a Dps family of DNA-binding proteins that is frequently encountered in bacterial genomes but rarely in phages, may also be involved in phage DNA replication. Gp67 is the only phiEco32 protein that belongs to a recognizable family of DNA-binding proteins.

Among phiEco32 replication proteins, gp33, gp53, gp74, and gp75 are most closely related to homologs from *P. aeruginosa* phage PaP3 (a close evolutionary relationship between these two phages of gammaproteobacteria is supported by analysis of several other phiEco32 genes; see Discussion). The remaining phiEco32 replication genes products show higher sequence similarity to various bacterial proteins, although the closest relative of putative phiEco32 thioredoxin (gp65) comes from phage T5.

PhiEco32 proteins involved in nucleotide metabolism—Phage genomes commonly encode enzymes of nucleotide salvage and modification.⁴ PhiEco32 codes for at least 4–5

proteins of this class--putative deoxynucleoside monophosphate kinase gp34, ADP-ribosylphosphate-processing phosphatase gp37, flavin-dependent thymidylate synthase gp64, thioredoxin-like protein gp65, and deoxycytidine triphosphate deaminase gp72. The phylogenetic affinities of these enzymes are different: closest gp34, gp37, and gp64 homologs come from three distinct families of tailed phages (siphovirus T1, myovirus phiKZ, and podovirus SiO1, respectively), gp72 is equally close to homologs from phiKZ and from cyanobacterium *Synechococcus elongates*, and gp65 contains a thioredoxin-like domain most closely related to proteins from *Fulvimarina pelagi* and other uncultured marine bacteria.

Structural proteins of phiEco32—We used mass-spectrometric analysis of purified virions to identify structural proteins of phiEco32. In one approach, virion components were separated by denaturing SDS-PAGE (Fig. 3), gel slices containing visible protein bands were treated with trypsin and digests were analyzed by ESI-MS/MS. Ten virion components, gp8, gp11, gp13-15, gp18-19, gp25-26, and gp58, were identified in this way (Fig. 3 and Table 1). Only six of these proteins have sequence similarities indicative of their structural roles, underscoring the importance of experimental analysis for comprehensive determination of the structural set of phage proteins.

Most gel bands contained more than one protein (Fig. 3). The predicted molecular masses of the proteins and their apparent molecular masses in the gel were in approximate agreement, with a notable exception of tail fiber protein gp15, which was a predominant component of two distinct bands: band 6/7 has an apparent molecular weight of 70 kDa, which is close to the predicted molecular weight of gp15 (77 kDa); band 1, however, has an apparent MW above 200 kDa. This might indicate that gp15 is modified post-translationally and/or forms very stable trimers that were not completely dissociated before SDS-PAGE. The thermal stability of the trimeric tailspike protein of P22-like phages has been well-documented.¹⁶

As expected for the most abundant virion component, the major capsid protein is also found in more than one band. The majority is found in band 9 (Fig. 3) but the 352 amino acid capsid protein is also a significant component of band 8, which has an apparent size about 20 kDa larger. A protein of this size could be synthesized via a -1 frameshift during translation of ORF11 making a gp11-12 fusion protein of 528 amino acids. Programmed frameshifting is a common feature in long-tailed double-stranded DNA phages¹⁷ and also in the T7 family.¹⁸ Near the end of the ORF11 reading frame a potential slippery sequence (GGGAAAG) is present in the mRNA, this is the same sequence found in phage λ that allows synthesis of the essential gpGT fusion protein at a level about 3.5% of the non-frameshifted gpG product.¹⁷ In phiEco32 ORF12 has a very weak Shine-Dalgarno element (Table 1) and is unlikely to be synthesized as an independent protein. However, a gp11-12 fusion protein would place the bacterial Ig-like domain of gp12 on the phage capsid, a location that similar domains are found at in many other phages¹⁹, including T7. In the latter phage family the coding sequence for the frameshifted, minor capsid protein gp10B, is immediately followed by a typical class II transcription terminator. A similar stem-loop and oligoU stretch immediately follows the coding sequence mRNA for the phiEco32 gp11-12 fusion protein.

Highly-purified phiEco32 particles were also examined by MudPIT, a shotgun proteomics approach that allows analysis of complex protein mixtures without electrophoretic separation. Peptides matching twenty of the phiEco32-encoded proteins could be identified. Nine of these proteins are shared with the set of structural proteins identified by gel band analysis and correspond to the most abundant proteins in phiEco32 virions. The other eleven proteins detected by MudPIT are of lesser abundance and of lower molecular weight. Most of these proteins would run between bands 11 and 12, a portion of the gel that has no stained material (Fig. 3). Seven of these lower-abundance proteins (gp20-22, gp24, and gp67-68) are conserved in other phages and bacteria, and the predicted functions of gp20, gp22, and gp24 are consistent

with their presence in the virions (Table 1). Other low-abundance proteins, such as the putative DNA-binding protein gp67, may be novel virion components, or their presence may be due to adventitious binding to virions.

Transcription regulation of phiEco32

The phiEco32 genome encodes a putative RNA polymerase (RNAP) σ factor, the product of gene 36. Gp36 is related to σ^{70} -like factors of the ECF subfamily. Proteins belonging to this very diverse subfamily typically recognize promoters of genes whose products participate in specialized cellular adaptations and responses to various external stresses (hence the name ECF, for extracytoplasmic factors, reviewed in Ref. 20). To determine if gp36 indeed functions as a σ factor, *E. coli* cells with chromosomally-encoded protein A (PrA)-tagged RNAP β' subunit were infected with phiEco32, RNAP was affinity-purified and its composition was compared to that of RNAP from uninfected cells. As can be seen from a gel presented in Fig. 4A, RNAP from infected cells contained two bands with apparent molecular masses of ~26 and ~10 kDa that were absent from the control lane. Mass spectrometric analysis revealed that the 26 kDa band was gp36 ($E = 4.9 \times 10^{-17}$), suggesting that this protein interacts with host RNAP, as expected of a σ factor. The 10 kDa band was identified as gp79 ($E = 4.2 \times 10^{-4}$), a small non-conserved protein of unknown function.

MudPIT analysis of PrA-tagged RNAP purified from uninfected and phiEco32-infected *E. coli* cells was also performed. In the uninfected sample, four different σ factors ($\sigma^{70}/\sigma^{24}/\sigma^{32}/\sigma^{38}$) were detected in substoichiometric amounts (Fig. 4B). In contrast, only low levels of the primary host sigma factor, σ^{70} , were identified in RNAP from infected cells. Two phage-specific proteins detected in gels, gp36 and gp79, were also found by MudPIT in this preparation, suggesting that one or both of these phage proteins may compete with endogenous σ factors for binding the RNAP core. In addition, the phiEco32 proteins gp98 and gp60 were detected in RNAP from infected cells. However, these two proteins were represented by single peptides and were present at lower levels; they may therefore be contaminants.

To validate the affinity purification results, the DNA encoding the two major phiEco32 proteins present in the RNAP preparation purified from infected cells, phiEco32 gp36 and gp79 were cloned in *E. coli* expression vectors, and recombinant proteins were purified and tested for their ability to bind to *E. coli* RNAP core. As can be seen from results of a native gel protein-protein interaction assay presented in Fig. 5, both gp36 and gp79 alone run off the gel (lanes 1 and 2), while RNAP core formed a characteristic slow-moving band²⁰ (lane 3). Addition of gp36 to the core resulted in formation of a new sharp band with higher mobility (lane 4), a situation observed upon the holoenzyme formation with other σ factors, see for example, Ref. 20; in fact the mobility of the new band matched that of the σ^{70} holoenzyme, data not shown. Likewise addition of gp79 resulted in a formation of a band that moved just slightly slower than the fast-moving band formed upon the addition of gp36 (lane 5). We conclude that both gp36 and gp79 can bind *E. coli* RNAP core *in vitro*, in agreement with affinity purification results, above.

A complex containing gp36 and RNAP core did not transcribe from a strong σ^{70} -dependent promoter T7 A1 (data not shown). The promoter specificity of the gp36-associated holoenzyme remains to be determined. Most likely, gp36 allows RNAP core to recognize those phiEco32 promoters that are distinct from early promoters that must be recognized by the σ^{70} holoenzyme. Recombinant gp79 efficiently inhibited promoter-dependent transcription by the σ^{70} holoenzyme (Fig. 6). Thus, gp79 may be a host transcription shut-off factor. The molecular mechanism of transcription inhibition by gp79 and the physiological role of this protein will be the subject of future investigations.

DISCUSSION

We report the isolation and initial characterization of phiEco32, a novel podophage infecting *E. coli*. The C3 type morphology of phiEco32 virions is quite rare, occurring in <1% of phage virions²²; curiously, one of the first phages ever observed by electron microscopy^{23,24} also had C3 morphology. The closest known morphological relatives of phiEco32 are *Salmonella enterica* serotype Newport phage 7-11²⁵, coliphage Esc-7-11²⁶, *Lactococcus lactis* phage KSY1²⁷, and *Vibrio vulnificus* phage 71A-6.²⁸ Phage Esc-7-11 has a head of 134 × 40–44 nm and its genome has been estimated to be 70.5 kbp.²⁹ No sequence information is available for salmonellaphage 7-11. The genome sizes of salmonellaphage 7-11 and vibriophage 71A-6 have been estimated to be 93 and 143 kbp, respectively.^{30,31} No evidence for variation in phiEco32 head size, which is quite common in salmonellaphage 7-11, was found, suggesting that the two phages are distinct. The genome sizes of the *Lactococcus* phage KSY1 (79,232 bp) and phiEco32 (77,554 bp) are similar, but KSY1 differs from phiEco32 by genome sequence and structure, larger head (233 × 45 nm), elaborate fixation structures, and host range.

The 54 conserved ORFs in the phiEco32 genome encode proteins whose best matches in public databases come from a diverse set of bacteriophages and bacteria. Thus, the phiEco32 genome is a complex mosaic, a situation encountered with many other phages. Fourteen of the 54 conserved phiEco32 ORFs have proteins encoded by *P. aeruginosa* bacteriophage PaP3 as closest database relatives (Table 1, Fig. 7); four additional phiEco32 proteins have significant sequence similarity to PaP3 ORFs, two among these being the second-closest matches, with scores insignificantly lower than those of the best matches. Similar to phiEco32, the coding regions of PaP3 are divided into two oppositely transcribed groups. Within each PaP3 group, clusters of genes whose products show significant similarities to phiEco32 proteins are present (Fig. 2). The first cluster encodes nine phiEco32 proteins (gp7, gp8, gp10, gp11, gp13, gp17, gp18, gp19, and gp24), mostly involved in head assembly and DNA packaging. The second cluster encodes seven proteins, two of which, gp74 and gp75, are enzymes involved in DNA replication (two additional components of the DNA replication assembly, gp33 and gp53, also have closely related homologs in PaP3 but are located outside of this cluster). Five more proteins in the second cluster, gp77, gp80, gp83, gp84, and gp86, contain several conserved domains indicative of various enzymatic functions (Table 1). The preservation of this module between phiEco32 and PaP3 is in stark contrast with numerous gene insertions and deletions observed in other parts of the two genomes. A comparison of all putative proteins with predicted functional or structural roles in the two phages indicate that PaP3 genes form an almost perfect subset of phiEco32 genes. Only PaP3 proteins p14 and p25 do not appear to have homologs in the phiEco32 genome. Structural proteins in phiEco32 for which no homologs are seen in PaP3 include a bacterial Ig-like domain (gp12 or the gp11-12 fusion), and tail fiber proteins (gp14-15). PaP3 is a temperate phage of *P. aeruginosa* isolated from hospital sewage¹¹. It is a member of *Podoviridae* owing to the presence of an icosahedral head, a short tail, and a linear dsDNA genome. However, the head of PaP3 is isometric and thus is clearly different from that of phiEco32. PaP3 is also a temperate phage, that has 5'-protruding cohesive ends and a genome (45,503 bp) that is much smaller than the phiEco32 genome. As phiEco32 also differs in that it has blunt ends with direct repeat, packaging and likely the mechanism of replication are therefore also different.

The phiEco32 genome encodes more proteins involved in replication and control of gene expression than the PaP3 genome. The phiEco32 genome encodes an RNAP σ factor, gp36. Several phages, including the well-studied coliphage T4, are known to encode proteins that recruit the host RNAP core to promoters of late viral genes. However, these proteins are only very distantly related to σ factors of the σ^{70} family. To date, only one phage, *B. anthracis* Fah, has been shown to encode a *bona fide* σ factor with all four conserved regions characteristic of proteins of this family.³² PhiEco32 gp36 is also an unmistakable homolog of σ factors of

the ECF subfamily. Gp36 binds host RNAP core and can displace the σ^{70} subunit from the holoenzyme *in vitro* (data not shown). Given the conservation of main domains characteristic of σ factors, the role of gp36 is unlikely to be limited to σ^{70} displacement; it is more likely that gp36-holoenzyme recognizes promoters of middle or late genes of the virus. Identification of these promoters will have to await the results of currently ongoing analysis of phiEco32 gene expression at various stages of transcription. Another phiEco32 protein that associates with host RNAP core is gp79, a novel transcription factor that inhibits σ^{70} -dependent transcription *in vitro*. This protein may inhibit early phage (and host) transcription and/or help gp36 to effectively compete with σ^{70} for a common core-binding site. Identification of the RNAP site that gp79 binds to and determination of the molecular mechanisms of transcription inhibition may clarify the physiological role of this novel transcription inhibitor.

MATERIALS AND METHODS

Isolation and propagation of phiEco32

PhiEco32 was isolated in 2004 from the river Kura, in Tbilisi, Georgia by enrichment on an *E. coli* 55 strain recovered from cows suffering from mastitis. PhiEco32 was propagated in laboratory in rich medium using its natural host *E. coli* 55. Clarified lysates were concentrated by PEG and then purified by equilibrium CsCl density gradients.

Electron microscopy

Density-gradient purified phages were deposited on a grid with a carbon-coated Formvar film, negatively stained with 2 % potassium phosphotungstate (pH 7.0), and examined in a Philips EM300 electron microscope operated at 60 kV. Magnification was controlled with T4 phage tails (length 113 nm).

Sequence analysis

ORFs of the phiEco32 genome were predicted using the GeneMark server (http://exon.gatech.edu/GeneMark/heuristic_hmm2.cgi31) and Glimmer2.³⁴ The PSI-BLAST program was used to detect the homologs of phiEco32 genes in the DNA and protein databases, with profile inclusion cutoff e-value in PSI-BLAST (-h parameter) set to 0.02. Both options of low-complexity filtering (-F parameter) and composition-based statistics (-t parameter) were sometimes adjusted during sequence similarity searches. tRNA genes were searched using the tRNAscan-SE server (<http://selab.janelia.org/tRNAscan-SE/35>).

The codon frequencies for phiEco32 and *E. coli* (NC_000913) genomes were calculated using the EMBOSS package.³⁶

Strain construction and purification of PrA-tagged RNAP

A strain of *E. coli* 55 encoding four Fc-binding repeats of the protein A (4PrA affinity tag³⁷) appended to the 3' end of the *rpoC* (RNAP β') gene was constructed using the method of gene gorging.³⁸ The presence of the PrA tag was validated by both PCR analysis of genomic DNA and Western blot analysis of cell lysates. The *E. coli* 55 wild-type and *E. coli* 55 *rpoC::4PrA* strains exhibited almost identical growth curves in rich medium and were productively infected by phiEco32 (data not shown).

To prepare phiEco32-infected biomass, wild-type *E. coli* 55 or *E. coli* 55 *rpoC::4PrA* strains were grown at 37 °C in 4 l of LB until an $A_{600\text{ nm}}$ of 0.5 and were infected with phiEco32 at a multiplicity of infection of 10. Infection was halted 23 minutes post-infection by rapidly cooling the samples in icy water baths. Cells were harvested by centrifugation and washed once with ice-cold 10 % (v/v) glycerol. Finally, 1 ml of 20 mM Hepes (pH 7.4 at 4 °C) supplemented with 0.2 mg/ml PMSF, 4 $\mu\text{g/ml}$ pepstatin was added per 10 g of cell paste, and

cells were frozen in liquid nitrogen. Cells were lysed by cryogenic grinding using the Retsch MM 301 Mixer Mill (Retsch). Eight 2-min bursts of grinding (30 Hz) with 20 mm tungsten carbide grinding balls were performed in 25 ml jars. The jars were cooled in liquid nitrogen between each step.

Lysed cells (1 g) were suspended in 5 ml of extraction buffer (20 mM Hepes (pH 7.4), 2 mM MgCl₂, 150 mM NaCl, 0.1 % (v/v) Tween 20, 0.2 mg/ml PMSF, 4 µg/ml pepstatin) supplemented with one protease inhibitor cocktail tablet (Roche Diagnostics). The lysate was treated with 300 Kunitz units of DNase I (Sigma-Aldrich) and 300 Kunitz units of RNase A (Sigma-Aldrich) at room temperature for 15 minutes with gentle agitation. Two successive 10-min centrifugation steps at 27,200 g were used to isolate the soluble fraction. The soluble fraction was incubated with 20 mg of Dynabeads (Invitrogen) cross-linked to rabbit IgG (MP Biomedicals) with gentle agitation for 5 minutes. Dynabeads were collected with a magnet and washed five times with wash buffer (20 mM Hepes (pH 7.4), 150 mM NaCl, 0.1 % (v/v) Tween 20). The β¹-4PrA fusion protein and co-purifying proteins were eluted from the IgG-Dynabeads with 0.5 M NH₄OH, 0.5 mM EDTA. The eluted proteins were frozen in liquid nitrogen and evaporated to dryness in a SpeedVac (Thermo Savant). Dried protein samples were dissolved in SDS-PAGE loading buffer and heated to 95 °C for 5 minutes. Iodoacetamide (25 mM) was added and the mixture incubated at room temperature to modify reduced cysteines. Samples were resolved by SDS-PAGE in 4–12 % (w/v) Bis-Tris polyacrylamide gels (Invitrogen). Proteins in the gel were visualized by Colloidal Coomassie staining with Gel Code Blue (Pierce).

Liquid chromatography and electrospray ionization mass spectrometry analysis of phiEco32 virion proteins

PhiEco32 virions were heated to 95 °C for 2.5 minutes, treated with DNase I (0.3 Kunitz units; Sigma-Aldrich) for 15 minutes at room temperature, mixed with SDS-PAGE sample buffer, and heated to 95 °C for a further 2.5 minutes. The sample was treated with iodoacetamide (25 mM) at room temperature, resolved on a denaturing 4–12 % (w/v) Bis-Tris polyacrylamide gel (Invitrogen), and stained with Gel Code Blue (Pierce). Stained bands were excised, destained, and digested as described above. The resulting peptides were loaded onto a microcolumn packed with Poros 20R2 reverse phase resin (PerSeptive Biosystems), washed, and eluted in two steps using (i) 5 pmol MFL tripeptide in 25% (v/v) acetonitrile, 0.1% trifluoroacetic acid and (ii) 5 pmol MFL tripeptide in 90 % (v/v) acetonitrile, 0.1 % (v/v) trifluoroacetic acid. The eluates were pooled and evaporated to dryness in a SpeedVac (Thermo Savant). The resulting tryptic peptide samples were resuspended in water/methanol/acetic acid at 44:5:1 (v/v/v) and loaded onto a Magic MS C₁₈ column (Michrom Bioresources). Peptides were separated using a methanol gradient from 10–100% in 9 minutes on a Smart System HPLC (GE Healthcare). The chromatographic eluate was directly infused at a rate of 2.1 µl/minute into an LCQ-Deca electrospray-ion trap mass spectrometer (Thermo Electron) through a 25 µm tapered-tip fused silica capillary. Ions were formed by an applied potential of +3.6kV and desolvation was assisted by maintaining the heated capillary at 135 °C and the use of a declustering potential of 40V across the tube lens. MS peaks above a signal threshold of 10⁵ in MS mode were subsequently fragmented using the following parameters: three micro scans, automatic gain control set to 500ms or a maximal number of counts of 5×10⁹, isolation window of 4 m/z units and relative collision energy of 35% (Thermo Electron nomenclature). MS/MS information was collected into separate files which were converted to DTA format using *extract_msn.exe* from Thermo Electron prior to database search.

Preparation of samples and MALDI MS mass spectrometry

Gel bands due to gp36 and gp79 were excised, destained, and digested with 25 ng/µl sequencing grade modified trypsin (Promega). Peptides were extracted on reverse phase resin (Poros 20

R2; PerSeptive Biosystems); eluted with 50 % (v/v) methanol, 20 % (v/v) acetonitrile, 0.1 % (v/v) trifluoroacetic acid and subjected to MALDI-MS analysis using an in-house constructed MALDI interface coupled to a Qq-TOF mass analyzer (Centaur, Sciex) and MALDI-MS/MS analysis using an in-house modified ion trap (LCQ DECA XP Plus, Thermo Electron).^{39,40} Proteins were identified using the algorithms “Profound”⁴¹ and “SonarMSMS”.⁴²

Mass spectrometry analysis of phiEco32 virion proteins

The TCA-precipitated protein pellet from phage virion preparation was denatured, reduced, alkylated, and digested with endoproteinase LysC and trypsin (both from Roche Applied Science, Indianapolis, IN) as described.⁴³ The peptide mixture was desalted offline on SPEC-PLUS PTC18 cartridges (Varian, Palo Alto, CA) and pressure-loaded onto a 100 μ m fused silica column packed with 9 cm AQUA C18 reverse phase (Phenomenex, Torrance, CA) and 3 cm of strong cation exchange material (Whatman, Brentford, UK).⁴⁴ The loaded and washed microcapillary column was installed in-line with a Quaternary 1100 series HPLC pump (Agilent Technologies, Santa Clara, CA), coupled to Deca-XP ion trap tandem mass spectrometer (ThermoElectron, San Jose, CA) and analyzed via a ten-step chromatography as described.⁴³

The MS/MS datasets were searched using SEQUEST⁴⁵ against a database combining 133 phiEco32 proteins, 29823 sequences from six *E. coli* genomes (CFT073, K12, O157H7_EDL933, O157H7, UTI89, W3110) downloaded from NCBI in July 2006, 177 sequences for usual protein contaminants, as well as randomized sequences for each of the non-redundant entries (*i.e.* the final database size was 60266 amino acid sequences). DTASelect/CONTRAST⁴⁶ was used to select spectra/peptide matches with normalized difference in cross-correlation score (DeltCn) of at least 0.08, a minimum cross-correlation score (XCORR) of 1.8 for singly charged, 2.5 for doubly charged, and 3.5 for triply charged spectra, a maximum Sp rank of 10. In addition, peptides had to be fully tryptic and at least seven amino acids long. No peptide matching shuffled protein sequences passed this criteria set. Spectral counts were normalized against protein length⁴⁷ and NSAF values were used to estimate relative protein levels in the samples.

Cloning, overexpression, and purification of phiEco32 gp36 and gp79

The DNA encoding phiEco32 gp36 was cloned in two steps. Firstly, the DNA encoding phiEco32 gp36 was PCR amplified using primers that appended *NdeI* and *HindIII* sites at the 5' and 3' ends of gene 36, respectively. The resultant PCR product was cleaved with *NdeI* and *HindIII* and a DNA fragment encoding gene 36 nucleotides 241–648 cloned between the *NdeI* and *HindIII* sites of a pET28a-based plasmid, creating pSKB2phiEco32gp36#1. pSKB2phiEco32gp36#1 was next cleaved with *NdeI* and a PCR product encoding gene 36 nucleotides 1–240, cleaved with *NdeI*, was cloned between the *NdeI* site of pSKB2phiEco32gp36#1, creating pSKB2phiEco32gp36. The DNA encoding phiEco32 gp79 was amplified using primers that appended *NdeI* and *BamHI* sites at the 5' and 3' ends of gene 79, respectively. The PCR product was cleaved with *NdeI* and *BamHI* and cloned between the *NdeI* and *BamHI* sites of a pET28a-based plasmid, creating pSKB2phiEco32gp79. All DNA manipulations were confirmed to be correct by sequencing.

To express gp36, *E. coli* BL21(DE3) cells ([F⁻ *ompT hsdS_B(r_B⁻ m_B⁻) gal dcm* (DE3)]) carrying pSKB2phiEco32gp36 and pG-KJE8 (*dnaK-dnaJ-grgE, groES-groEL* (Takara BIO Inc., Japan)) plasmids were grown at 30°C in 300 ml LB with 50 μ g/ml of kanamycin and 40 μ g/ml of chloramphenicol. To induce chaperone synthesis L-arabinose (4 mg/ml) and tetracycline (10 ng/ml) were added to the medium. When the culture reached mid-log phase, expression of recombinant protein was induced by the addition of 0.1 mM IPTG and growth was continued for additional 2 h. Cells were harvested by centrifugation and resuspended in 9 ml of buffer A

(20 mM phosphate buffer, pH 7.4, 50 mM NaCl) with 1 mg/ml lysozyme. After a 1-hour incubation on ice, cells were disrupted by sonication. Cleared cell lysate was applied on a 1 ml heparin-agarose column connected to a 1 ml chelating HiTrap column (both from GE Healthcare) charged with Ni²⁺. Material bound to the HiTrap column was washed with buffer B (20 mM phosphate buffer, pH 7.4, 0.5 M NaCl, 50 mM imidazole) and bound proteins were eluted with buffer A containing 250 mM imidazole. Fractions containing gp36 were concentrated on Centricon® Centrifugal Filter Units (Millipore), glycerol was added to a final concentration 50% and protein was stored at -20 °C.

Gp79 expression was carried out in *E. coli* BL21(DE3) cells carrying pSKB2phiEco32gp79 and pG-KJE8 plasmids. Cell growth conditions and protein purification protocol were the same as for gp36 but without preliminary purification on a heparin-agarose column.

***In vitro* transcription**

His-tagged *E. coli* RNAP core and untagged recombinant σ^{70} subunit were prepared as described.⁴⁸

Abortive initiation transcription reactions were performed in 10 μ l of transcription buffer (40 mM Tris-HCl, 40 mM KCl, 10 mM MgCl₂, 5 mM DTT, 100 μ g/ml BSA) and contained 150 nM *E. coli* RNAP core enzyme, 300 nM recombinant σ^{70} and 600 nM of recombinant phiEco32 gp36 or gp79. Reactions were incubated for 15 min at 37 °C, followed by the addition of 20 nM of a PCR fragment containing the T7 A1 promoter, 100 μ M initiating dinucleotide CpA, 10 μ M of α -[³²P]UTP (400 Ci/mmol). Reactions proceeded for 10 min at 37 °C and were terminated by the addition of an equal volume of denaturing loading buffer. The reaction products were resolved on a denaturing 6 M urea 20% (w/v) polyacrylamide gels and visualized using a PhosphorImager.

Protein complex analysis

12 pmol of *E. coli* RNAP core was incubated with 100 pmol of gp36 or 60 pmol of gp79 in 40 μ l of transcription buffer for 10 min at 37 °C. Reaction products were separated by electrophoresis in a 5% native polyacrylamide gel (29:1) at 100 V for 1 h. The gel was stained with Coomassie G-250. The peptide composition of native-gel bands was established by SDS PAGE

Acknowledgements

This work was supported by NIH R01 grant GM59295, a new groups grant from the Presidium of Russian Academy of Sciences and a Russian Foundation for Basic Research grant (to KS), NIH R01 GM32095 grant (to IJM) and NIH grants RR00862 and RR022220 (to BTC). LFW was supported by an NIH grant GM61898 to Seth Darst.

REFERENCES

1. Hendrix RW, Smith MC, Burns RN, Ford ME, Hatfull GF. Evolutionary relationships among diverse bacteriophages and prophages: all the world's a phage. *Proc. Natl. Acad. Sci. USA* 1999;96:2192–2197. [PubMed: 10051617]
2. Wommack KE, Colwell RR. Virioplankton: viruses in aquatic ecosystems. *Microbiol. Mol. Biol. Rev* 2000;64:69–114. [PubMed: 10704475]
3. Hendrix RW. Bacteriophage genomics. *Curr. Opin. Microbiol* 2003;6:506–511. [PubMed: 14572544]
4. Liu J, Glazko G, Mushegian A. Protein repertoire of double-stranded DNA bacteriophages. *Virus Res* 2006;117:68–80. [PubMed: 16490276]
5. Pedulla ML, Ford ME, Houtz JM, Karthikeyan T, Wadsworth C, Lewis JA, Jacobs-Sera D, Falbo J, Gross J, Pannunzio NR, Brucker W, Kumar V, Kandasamy J, Keenan L, Bardarov S, Kriakov J,

- Lawrence JG, Jacobs WR Jr, Hendrix RW, Hatfull GF. Origins of highly mosaic mycobacteriophage genomes. *Cell* 2003;113:171–182. [PubMed: 12705866]
6. Naryshkina T, Liu J, Florens L, Swanson SK, Pavlov AR, Pavlova NV, Inman R, Minakhin L, Kozyavkin SA, Washburn M, Mushegian A, Severinov K. Thermus thermophilus bacteriophage phiYS40 genome and proteomic characterization of virions. *J. Mol. Biol* 2006;364:667–677. [PubMed: 17027029]
 7. Semenova E, Djordjevic M, Shraiman B, Severinov K. The tale of two RNA polymerases: transcription profiling and gene expression strategy of bacteriophage Xp10. *Mol. Microbiol* 2005;55:764–777. [PubMed: 15661002]
 8. Nechaev S, Severinov K. Bacteriophage-induced modifications of host RNA polymerase. *Annu. Rev. Microbiol* 2003;57:301–322. [PubMed: 14527281]
 9. Ackermann H-W, Eisenstark A. The present state of phage taxonomy. *Intervirology* 1974;3:201–219. [PubMed: 4461697]
 10. Casjens SR, Gilcrease EB, Winn-Stapley DA, Schicklmaier P, Schmieger H, Pedulla ML, Ford ME, Houtz JM, Hatfull GF, Hendrix RW. The generalized transducing Salmonella bacteriophage ES18: complete genome sequence and DNA packaging strategy. *J. Bacteriol* 2005;187:1091–1104. [PubMed: 15659686]
 11. Tan Y, Zhang K, Rao X, Jin X, Huang J, Zhu J, Chen Z, Hu X, Shen X, Wang L, Hu F. Whole genome sequencing of a novel temperate bacteriophage of *P. aeruginosa*: evidence of tRNA gene mediating integration of the phage genome into the host bacterial chromosome. *Cell. Microbiol* 2006;9:479–491. [PubMed: 16965514]
 12. Sacerdot C, Fayat G, Dessen P, Springer M, Plumbridge JA, Grunberg-Manago M, Blanquet S. Sequence of a 1.26-kb DNA fragment containing the structural gene for *Escherichia coli* initiation factor-IF3 – presence of an AUU initiator codon. *EMBO J* 1982;1:311–331. [PubMed: 6325158]
 13. Binns N, Masters M. Expression of the *Escherichia coli* *pcnB* gene is translationally limited using an inefficient start codon: a second chromosomal example of translation initiated at AUU. *Mol. Microbiol* 2002;44:1287–1298. [PubMed: 12068810]
 14. Nikolaou C, Almirantis Y. A study on the correlation of nucleotide skews and the positioning of the origin of replication: different modes of replication in bacterial species. *Nucleic Acids Res* 2005;33:6816–6822. [PubMed: 16321966]
 15. Miller ES, Kutter E, Mosig G, Arisaka F, Kunisawa T, Ruger W. The bacteriophage T4 genome. *Microbiol. Mol. Biol. Rev* 2003;67:86–156. [PubMed: 12626685]
 16. Chen B, King J. Thermal unfolding pathway for the thermostable P22 tailspike endorhamnosidase. *Biochemistry* 1991;30:6260–6269. [PubMed: 2059632]
 17. Xu J, Hendrix RW, Duda RL. Conserved translational frameshift in dsDNA bacteriophage tail assembly genes. *Mol. Cell* 2004;16:11–21. [PubMed: 15469818]
 18. Molineux, IJ. The T7 group. In: Calendar, R., editor. *The Bacteriophages*. Oxford University Press; 2005. p. 277–301.
 19. Fraser JS, Yu Z, Maxwell KL, Davidson AR. Ig-like domains on bacteriophages: a tale of promiscuity and deceit. *J. Mol. Biol* 2006;359:496–507. [PubMed: 16631788]
 20. Helmann JD. The extracytoplasmic function (ECF) sigma factors. *Adv. Microb. Physiol* 2002;46:47–110. [PubMed: 12073657]
 21. Severinova E, Severinov K, Fenyo D, Chait BT, Brody ET, Darst SA. Domain organization of the σ^{70} subunit of *Escherichia coli* RNA polymerase. *J. Mol. Biol* 1996;263:637–647. [PubMed: 8947564]
 22. Ackermann H-W. Frequency of morphological phage descriptions in the year 2000. *Arch. Virol* 2001;146:843–857. [PubMed: 11448025]
 23. Ruska H. Morphologische Befunde bei der bakteriophagen Lvse. *Arch. Gesamte Viruforsch* 1942;2:345–387.
 24. Kottmann R. Morphologische Befunde aus taches vierges von Colikulturen. *Arch. Gesamte Virusforsch* 1942;2:388–396.
 25. Moazamie N, Ackermann H-W, Murthy MRV. Characterization of two *Salmonella newport* bacteriophages. *Can. J. Microbiol* 1979;25:1063–1072. [PubMed: 540262]

26. Ackermann H-W, Nguyen T-M, Del ge R. Un nouveau phage d'ent robact ries   t te allong e et queue courte. *Ann Virol (Inst. Pasteur)* 1981;132E:229–234.
27. Chopin A, Deveau H, Ehrlich SD, Moineau S, Chopin M-C. KSY1, a lactococcal phage with a T7-like transcription. *Virology* 2007;365:1–9. [PubMed: 17467024]
28. DePaola A, Motes ML, Chan AM, Suttle CA. Phages infecting *Vibrio vulnificus* are abundant and diverse in oysters (*Crassostrea virginica*) collected from the Gulf of Mexico. *Appl. Environ. Microbiol* 1998;64:346–351. [PubMed: 9435088]
29. Grimont F, Grimont PAD. DNA relatedness among bacteriophages of the morphological group C3. *Curr. Microbiol* 1981;6:65–69.
30. Grimont F, Grimont PAD. Characteristics of five bacteriophages of yellow-pigmented enterobacteria. *Curr. Microbiol* 1981;5:61–66.
31. Khan AS, Khan AA, Nawaz MS, DePaola A, Andrews A, Cerniglia CE. DNA packaging and developmental intermediates of a broad host range *Vibrio vulnificus* bacteriophage 71A-6. *Mol. Cell. Probes* 2001;15:61–69. [PubMed: 11292322]
32. Minakhin L, Semenova E, Liu J, Vasilov A, Severinova E, Gabisonia T, Inman R, Mushegian A, Severinov K. Genome and gene expression of *Bacillus anthracis* bacteriophage Fah. *J. Mol. Biol* 2005;354:1–15. [PubMed: 16226766]
33. Besemer J, Borodovsky M. Heuristic approach to deriving models for gene finding. *Nucleic Acid. Res* 1999;27:3911–3920. [PubMed: 10481031]
34. Delcher AL, Harmon D, Kasif S, White O, Salzberg SL. Improved microbial gene identification with GLIMMER. *Nucleic Acids Res* 1999;27:4636–4641. [PubMed: 10556321]
35. Lowe TM, Eddy SR. tRNAscan-SE: a program for improved detection of transfer RNA genes in genomic sequence. *Nucleic Acids Res* 1997;25:955–964. [PubMed: 9023104]
36. Rice P, Longden I, Bleasby A. EMBOSS: The European Molecular Biology Open Software Suite. *Trend. Genetics* 2000;16:276–277.
37. Tackett AJ, Dilworth DJ, Davey MJ, O'Donnell M, Aitchison JD, Rout MP, Chait BT. Proteomic and genomic characterization of chromatin complexes at a boundary. *J. Cell Biol* 2005;169:35–47. [PubMed: 15824130]
38. Herring CD, Glasner JD, Blattner FR. Gene replacement without selection: regulated suppression of amber mutations in *Escherichia coli*. *Gene* 2003;311:153–163. [PubMed: 12853150]
39. Krutchinsky AN, Zhang W, Chait BT. Rapidly switchable matrix-assisted laser desorption/ionization and electrospray quadrupole-time-of-flight mass spectrometry for protein identification. *J. Am. Soc. Mass Spectrom* 2000;11:493–504. [PubMed: 10833023]
40. Krutchinsky AN, Kalkum M, Chait BT. Automatic identification of proteins with a MALDI-quadrupole ion trap mass spectrometer. *Anal. Chem* 2001;73:5066–5077. [PubMed: 11721901]
41. Zhang W, Chait BT. ProFound: an expert system for protein identification using mass spectrometric peptide mapping information. *Anal. Chem* 2000;72:2482–2489. [PubMed: 10857624]
42. Field HI, Feny  D, Beavis RC. RADARS, a bioinformatics solution that automates proteome mass spectral analysis, optimises protein identification, and archives data in a relational database. *Proteomics* 2002;2:36–47. [PubMed: 11788990]
43. Florens L, Washburn MP. Proteomic analysis by multidimensional protein identification technology. *Methods Mol. Biol* 2006;328:159–175. [PubMed: 16785648]
44. Washburn MP, Wolters D, Yates JR III. Large-scale analysis of the yeast proteome by multidimensional protein identification technology. *Nat. Biotechnol* 2001;19:242–247. [PubMed: 11231557]
45. Eng J, McCormack AL, Yates JR III. An approach to correlate tandem mass spectral data of peptides with amino acid sequences in a protein database. *J. Amer. Mass Spectrom* 1994;5:976–989.
46. Tabb DL, McDonald WH, Yates JR III. DTASelect and Contrast: tools for assembling and comparing protein identifications from shotgun proteomics. *J. Proteome Res* 2002;1:21–26. [PubMed: 12643522]
47. Zybailov B, Mosley AL, Sardi  ME, Coleman MK, Florens L, Washburn MP. Statistical analysis of membrane proteome expression changes in *Saccharomyces cerevisiae*. *J. Proteome Res* 2006;5:2339–2347. [PubMed: 16944946]

48. Kashlev M, Nudler E, Severinov K, Borukhov S, Komissarova N, Goldfarb A. Histidine-tagged RNA polymerase of *Escherichia coli* and transcription in solid phase. *Methods Enzymol* 1996;274:326–334. [PubMed: 8902816]

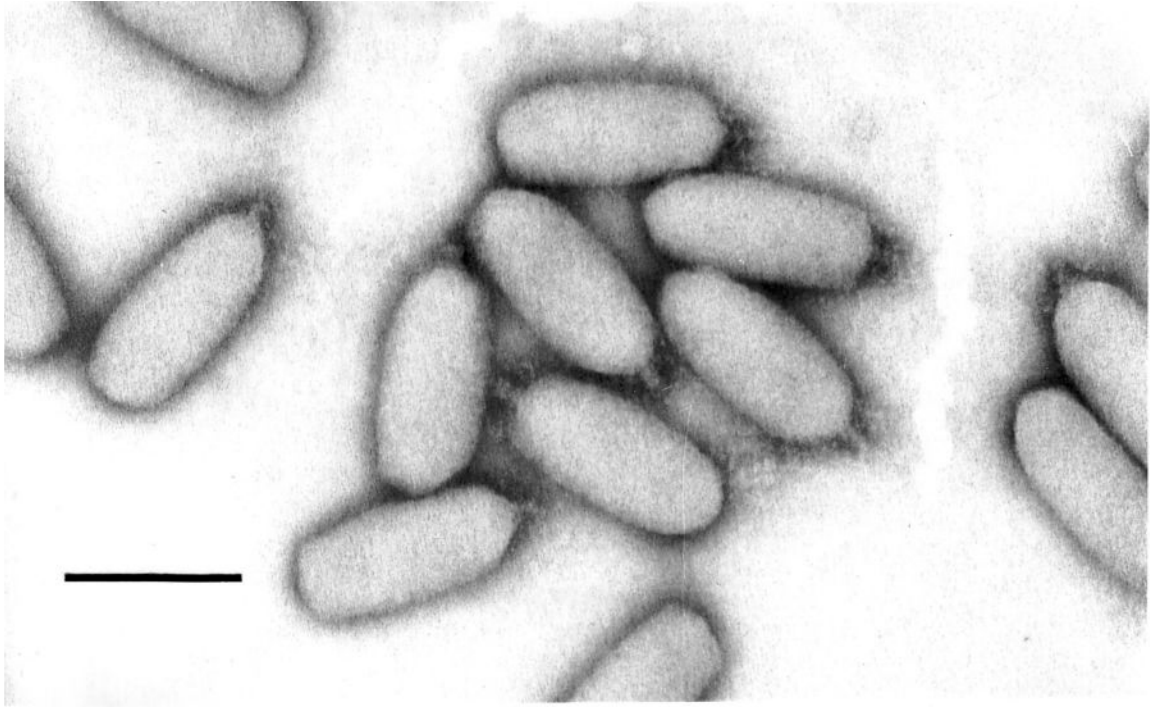


Figure 1. Morphology of phiEco32 virions

Phage phiEco32 virions stained with phosphotungstate and revealed by electron microscopy. Final magnification is $\times 297,000$; the bar represents 100 nm. The virions appear oval due to flattening of the central part of the capsid.

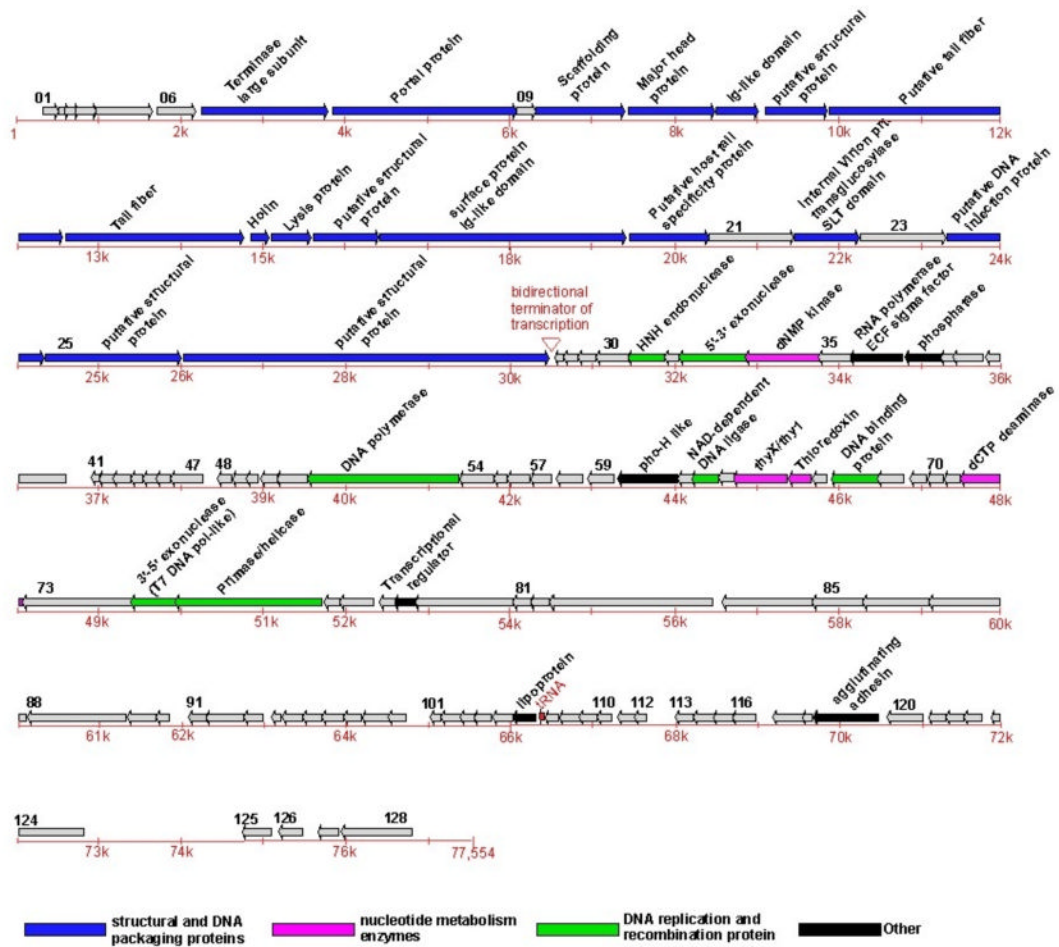


Figure 2. The phiEco32 genome

The phiEco32 genome is schematically presented with predicted ORFs indicated by arrows and numbered in black. The direction of an arrow indicates the direction of transcription. ORFs for whose products clear functional predictions can be made are highlighted by color (see Table 1 for more details); ORF79, which codes for a novel RNAP inhibitor identified in this work, is also indicated. The genes encoding phiEco32 virion proteins as identified by a combination of LC-ESI MS/MS and MudPIT are highlighted. The putative bidirectional terminator of transcription is indicated by a red wedge and the tRNA gene is also indicated by a red arrow and labeled in red. A scale of nucleotide numbers (red) runs below the ORFs.

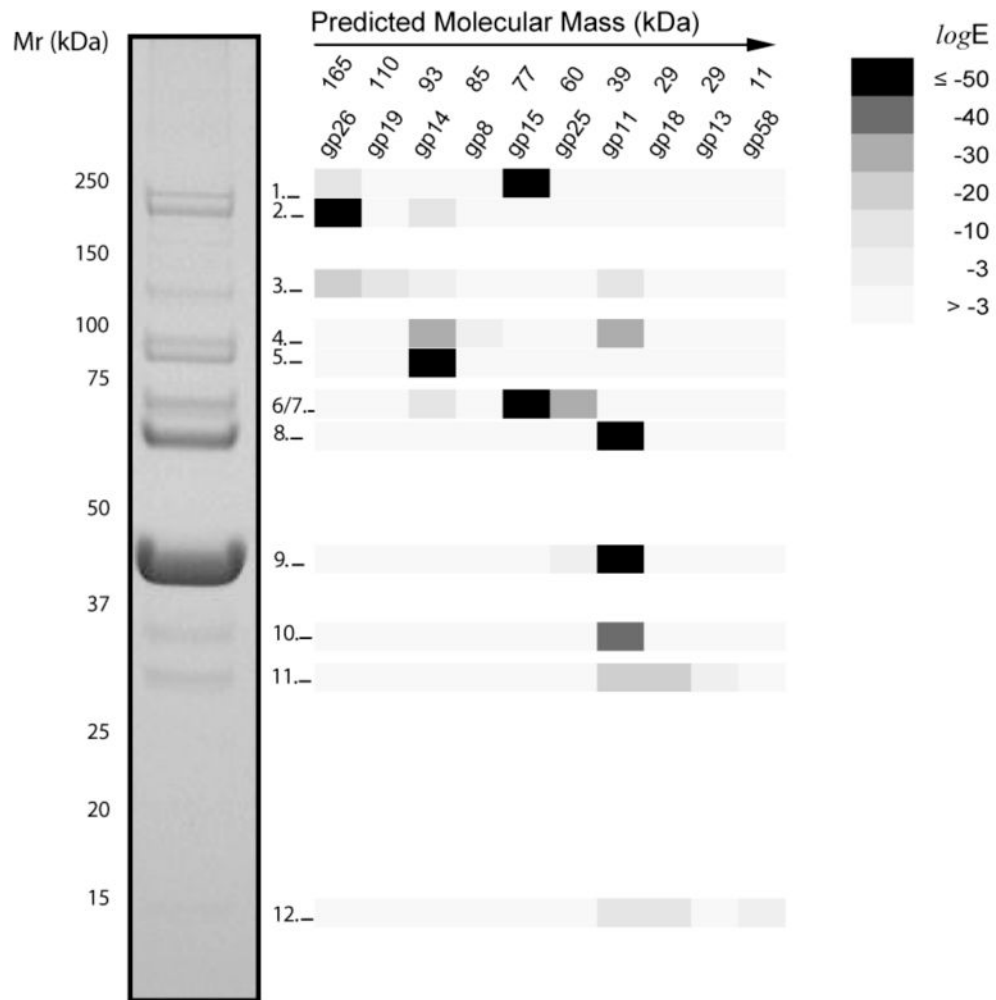


Figure 3. Mass spectrometric analysis of virion proteins

A highly purified preparation of phiEco32 virions was loaded onto a 4–12 % SDS-gel and after electrophoresis proteins were stained with Coomassie. Eleven bands were in-gel digested with trypsin and the resulting peptides were analyzed by LC/MS/MS. The proteins (identified by their “gp” number) detected in each band were plotted in a matrix coded by their expectation values as indicated. Numbers above the “gp” numbers are predicted molecular masses for each protein.

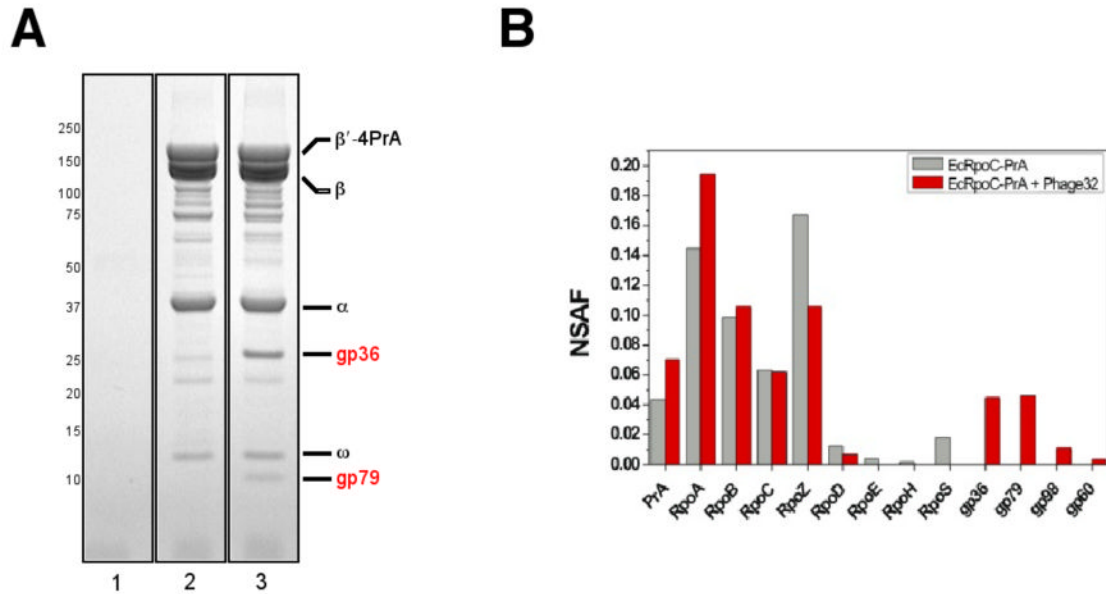


Figure 4. Polypeptide composition of RNAP affinity purified from phiEco32-infected cells
A. The β' -4PrA fusion protein, and co-isolating proteins, was affinity purified from *E. coli* 55 infected with phiEco32 (lane 1; control), *E. coli* 55*rpoC::4PrA* (lane 2), and *E. coli* 55*rpoC::4PrA* + phiEco32 (lane 3). The samples were analyzed by SDS-PAGE and bands due to proteins present in lane 3, but absent from lanes 1 and 2, were identified by MALDI MS.
B. NSAF values for proteins identified by MudPIT in RNAP samples affinity purified from both phiEco32-infected and uninfected cells are shown.

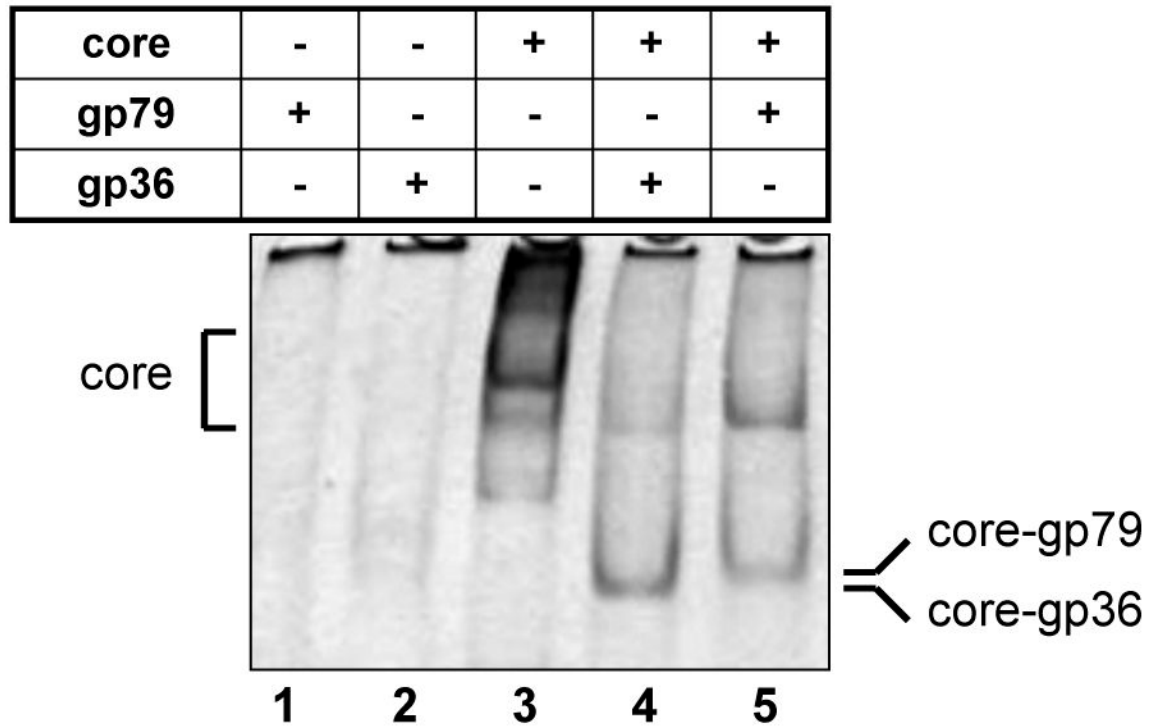


Figure 5. PhiEco32 gp36 and gp79 bind *E. coli* RNAP core *in vitro*
 The indicated proteins were combined and loaded on a native polyacrylamide gel. After electrophoresis complexes were revealed by Coomassie-staining.

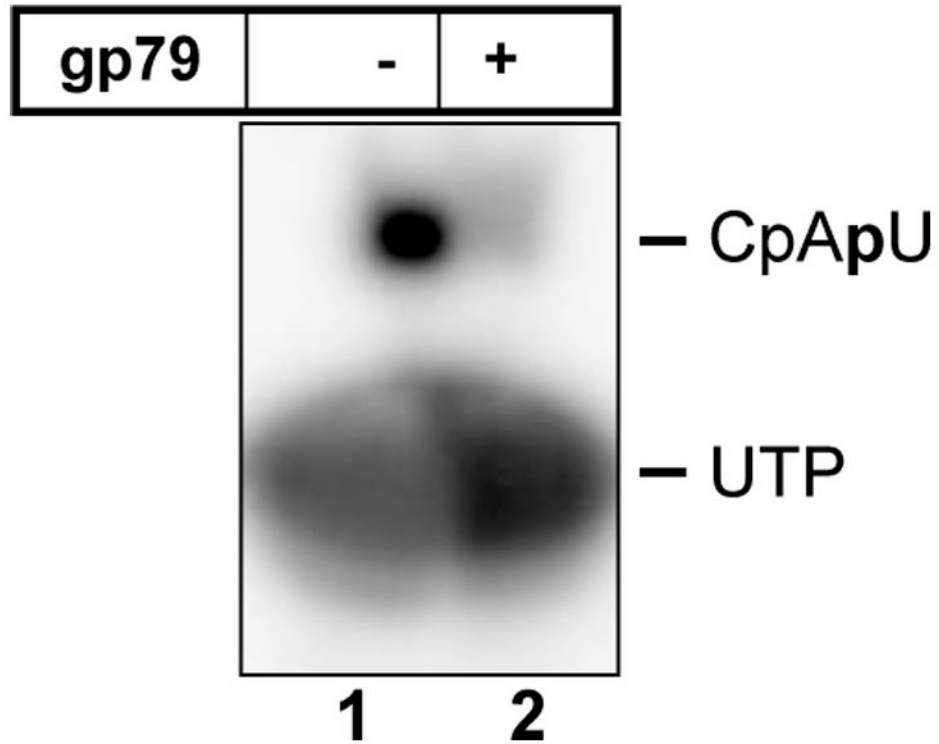


Figure 6. PhiEco32 gp79 inhibits abortive initiation by *E. coli* σ^{70} RNAP holoenzyme
The results of abortive synthesis of the CpApU product from CpA and radioactively labeled UTP from the T7 A1 promoter-containing fragment in the presence or in the absence of gp79 are presented.

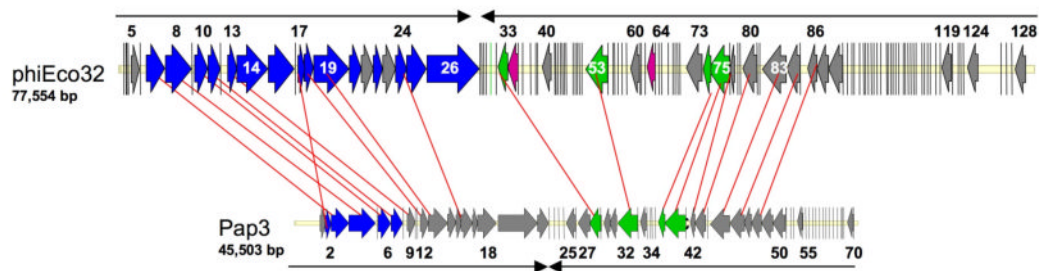


Figure 7. Comparison of phiEco32 and PaP3 genomes

The phiEco32 and PaP3 genomes are drawn to scale with larger ORFs indicated as arrows, the direction of an arrow indicating the direction of transcription. Smaller ORFs have been reduced to bars to avoid cluttering the figure. The ORFs in phiEco32 are colored according to the functional predictions made (Table 1, Fig. 2). The ORFs in PaP3 are colored with a similar scheme using the annotations from the Genbank entry NC_004466. The homologous genes in the two genomes are connected by red lines. The light yellow bar in both genomes indicates the whole length of the genome. The black arrows (on top in PhiEco32 and below in PaP3) indicate the direction of transcription of the ORFs in that region.

Table 1
Sequence similarity and predicted molecular function for gene products of phiEco32

ORF/Names	ORF strand/position ^a	ORF length (aa)	GenBank ID and taxonomic origin of the best database match	GeneBank ID and taxonomic origin of the best database match among phages (if different)	Predicted molecular function	Comments
1	296..496	66				Weak SD element
2	489..629	46				Weak SD element
3	565..744	59	77118167 <i>Escherichia coli</i> phage K1F			
4	698..952	84				
5	945..1640	231				
6	1697..2170	157				
7	2240..3781	513				
8	3843..6086	747		27414483 <i>Pseudomonas aeruginosa</i> phage PaP3	Terminase large subunit	
9	6096..6332	78		27476052 <i>Pseudomonas aeruginosa</i> phage PaP3	Portal protein	
10	6332..7417	361	27414480 <i>Pseudomonasaeruginosa</i> phage PaP3		Scaffolding protein	Weak SD element
11	7459..8517	352	78696363 <i>Bradyrhizobium</i> sp.	27414479 <i>Pseudomonas aeruginosa</i> phage PaP3	Major head protein	
12	8529..9041	170	90587664 <i>Flavobacterium johnsoniae</i>	27476047 <i>Pseudomonas aeruginosa</i> phage PaP3	Bacterial Ig-like domain	
13	9143..9895	250	113876452 <i>Shorhizobium medicae</i>		Conserved hypothetical protein	
14	9905..12547	880				
15	12588..14756	722	45686334 <i>Escherichia coli</i> phage T1		Putative tail fiber	
16	14849..15067	72	3370533 <i>Yersinia enterocolitica</i> phage PY54		Tail fiber	
17	15097..15588	163				Holin
18	15601..16404	267	33340418 <i>Salmonella</i> phage Felix01		Lysis protein (muraminidase)	
19	16414..19431	1005	52139914 <i>Escherichia coli</i> phage JS98		Putative structural protein	
20	19475..20443	322	27414473 <i>Pseudomonas aeruginosa</i> phage PaP3		Bacterial surface proteins containing Ig-like region	
21	20445..21476	343	77864687 <i>Burkholderia cepacia</i> phage Bcep176		Putative tail tip fiber protein and a host specificity determinant	
22	21489..22271	260	22126074 <i>Yersinia pestis</i>	33770532 <i>Yersinia enterocolitica</i> phage PY54	Conserved hypothetical protein	
23	22291..23343	350	29243594 <i>Pseudomonas putida</i> phage gh-1		Virion protein with transglycosylase SLT domain	
24	23356..24324	322	27476040 <i>Pseudomonas aeruginosa</i> phage PaP3		Putative DNA injection protein	
25	24338..25993	551				
26	26061..30482	1473				
27	-(30552..30659)	35				
28	-(30672..30833)	53				
29	-(30842..31069)	75				
30	-(31062..31460)	132				
31	-(31450..31902)	150	32453596 <i>Escherichia coli</i> phage RB69		Conserved hypothetical protein	
32	-(31889..32068)	59	149408178 <i>Pseudomonas aeruginosa</i> phage PA11		Conserved hypothetical protein	
			33340391 <i>Salmonella</i> phage Felix01		HNH endonuclease	Weak SD element

ORF/Names	ORF strand/position ^a	ORF length (aa)	GenBank ID and taxonomic origin of the best database match	GeneBank ID and taxonomic origin of the best database match among phages (if different)	Predicted molecular function	Comments
33	-(32082..32900)	272	27414457 <i>Pseudomonas aeruginosa</i> phage PaP3		5'-3' exonuclease similar to the N-terminal exonuclease domain of DNA polymerase I	
34	-(32887..33780)	297	45686300 <i>Escherichia coli</i> phage T1		ATP-binding protein with Walker A motif; an ATPase or dNMP kinase	
35	-(33777..34169)	130	88603084 <i>Methanospirillum hungatei</i>	3172310 Mycobacteria phage D29	Predicted GTP-binding protein	
36	-(34166..34810)	214	68229118 <i>Frankia sp.</i>		RNA polymerase ECF sigma factor	
37	-(34833..35273)	146	94498600 <i>Sphingomonas sp.</i>	29135040 <i>Pseudomonas aeruginosa</i> phage phiTKZ	Appr-1-p processing enzyme family, phosphatase	Weak SD element
38	-(35273..35446)	57	56412276 <i>Salmonella enterica</i>		Conserved hypothetical protein	No SD element
39	-(35418..35768)	116	33340399 <i>Salmonella</i> phage Felix01			
40	-(35826..36572)	248				
41	-(36883..36995)	35				
42	-(36989..37168)	59				
43	-(37149..37364)	71				
44	-(37380..37523)	47	71834082 <i>Escherichia coli</i> phage JK06			
45	-(37520..37687)	55				
46	-(37684..37860)	46				No SD element Match in an environmental sample, 44001214
47	-(37857..38249)	130				
48	-(38431..38607)	58				
49	-(38617..38784)	55				
50	-(38784..38912)	42	81343940 <i>Escherichia coli</i> phage RTP		Conserved hypothetical protein	
51	-(38968..39159)	63	5354344 <i>Escherichia coli</i> phage T4		Conserved hypothetical protein	
52	-(39159..39524)	121				
53	-(39533..41377)	614	27414453 <i>Pseudomonas aeruginosa</i> phage PaP3		DNA polymerase domain, lacking both 5'-3' and 3'-5' exonuclease domains.	
54	-(41394..41807)	137				
55	-(41809..41967)	52				
56	-(41971..42255)	94				
57	-(42257..42514)	85				
58	-(42583..42900)	105	40549402 <i>Pseudomonas aeruginosa</i> phage PaP3			
59	-(42955..43287)	110	58336433 <i>Lactobacillus acidophilus</i>	38640011 <i>Aeromonas hydrophila</i> phage Aeh1	Conserved hypothetical protein	
60	-(43318..44061)	247	29376909 <i>Enterococcus faecalis</i>	19343479 <i>Roseobacter</i> phage SIO1	Phosphate starvation-inducible phoH-like, ATPase	
61	-(44058..44243)	61				
62	-(44230..44559)	109	22298400 <i>Thermosynechococcus elongatus</i>	82657960 <i>Pseudomonas</i>	NAD-dependent DNA ligase, minimal nucleotidyltransferase	Weak SD element

ORF/Names	ORF strand/position ^a	ORF length (aa)	GenBank ID and taxonomic origin of the best database match	GeneBank ID and taxonomic origin of the best database match among phages (if different)	Predicted molecular function	Comments
63	– (44556..44741)	61		<i>aeruginosa</i> phage phiEL	domain as in some other phages and viruses	Weak SD element
64	– (44741..45397)	218	149408182 <i>Pseudomonas aeruginosa</i> phage PA11		Thymidylate synthase thyX/thy1 (flavin-dependent)	
65	– (45413..45688)	91	114705060 <i>Fulvimarina pelagi</i>	46401774 <i>Escherichia coli</i> phage T5	Thiol-disulfide isomerase and thioredoxin	
66	– (45697..45876)	59		56693168 <i>Lactobacillus plantarum</i> phage LP65	DNA-binding protein, DPS family of ferritin-like diiron-carboxylate proteins	
67	– (45937..46500)	187	88912807 <i>Acidothermus cellulolyticus</i>		Conserved hypothetical protein	Weak SD element Weak SD element
68	– (46493..46822)	109	34333203 <i>Vibrio</i> phage KVP40			
69	– (46895..47104)	69		18996679 <i>Pseudomonas aeruginosa</i> phage phiKZ	dCTP deaminase	
70	– (47104..47313)	69				
71	– (47313..47510)	65				
72	– (47511..48044)	177	56750822 <i>Synechococcus elongatus</i>			
73	– (48054..49367)	437				
74	– (49369..49926)	185	27414446 <i>Pseudomonas aeruginosa</i> phage PaP3		3'-5' exonuclease domain of type I DNA polymerase	Weak SD element
75	– (49920..51710)	596	27414445 <i>Pseudomonas aeruginosa</i> phage PaP3		Primase/helicase	
76	– (51737..51940)	67	15669708 <i>Methanocaldococcus jamaaschii</i>			
77	– (51930..52349)	139		27414443 <i>Pseudomonas aeruginosa</i> phage PaP3	Conserved YtfP/UPF0131 family, predicted FAD-binding oxidoreductase	Weak SD element
78	– (52419..52604)	61				
79	– (52601..52849)	82				
80	– (52856..54049)	397	149408167 <i>Pseudomonas aeruginosa</i> phage PA11		ATP-grasp enzyme, predicted amino acid ligase/glutaminyl transferase	
81	– (54052..54276)	74				
82	– (54257..54490)	77				
83	– (54493..56523)	676	149408163 <i>Pseudomonas aeruginosa</i> phage PA11		Glutamine amidotransferase domain AUU start codon	Weak SD element
84	– (56603..57706)	367	27414439 <i>Pseudomonas aeruginosa</i> phage PaP3			
85	– (57703..58320)	205				
86	– (58330..59136)	268	27414437 <i>Pseudomonas aeruginosa</i> phage PaP3			
87	– (59129..60100)	323				
88	– (60111..61310)	399				
89	– (61332..61684)	120				
90	– (61687..61839)	50				

ORF/Names	ORF strand/position ^a	ORF length (aa)	GenBank ID and taxonomic origin of the best database match	GeneBank ID and taxonomic origin of the best database match among phages (if different)	Predicted molecular function	Comments
91	-(62075..62290)	71	111116430 <i>Escherichia coli</i> APEC 01			Weak SD element
92	-(62290..62754)	154	32453588 <i>Escherichia coli</i> phage RB69		Conserved hypothetical protein	Weak SD element
93	-(62754..62987)	77				
94	-(63094..63210)	38				
95	-(63219..63467)	82				
96	-(63473..63718)	81				Weak SD element
97	-(63718..63966)	82				Weak SD element
98	-(63968..64198)	76				Weak SD element
99	-(64207..64530)	107				Weak SD element
100	-(64520..64741)	73				
101	-(65031..65162)	43				
102	-(65159..65404)	81				
103	-(65388..65561)	57	149408169 <i>Pseudomonas aeruginosa</i> phage PA11			
104	-(65571..65792)	73				
105	-(65800..66048)	82				
106	-(66050..66331)	93	81343973 <i>Escherichia coli</i> phage RTP		Putative phage lipoprotein	No SD element
107	-(66436..66615)	59				
108	-(66608..66859)	83	148734558 <i>Escherichia coli</i> phage TLS		Conserved hypothetical protein	
109	-(66856..67080)	74				
110	-(67077..67253)	58				
111	-(67332..67541)	69				
112	-(67531..67671)	46	33340411 <i>Salmonella</i> phage Felix 01		Conserved hypothetical protein	Weak SD element
113	-(68030..68248)	72				Weak SD element
114	-(68249..68506)	85				Weak SD element
115	-(68496..68732)	78				
116	-(68722..69018)	98				
117	-(69218..69607)	129				
118	-(69582..69713)	43				Weak SD element
119	-(69718..70515)	265	16565696 <i>Escherichia coli</i>		Agglutinating adhesin	Weak SD element
120	-(70617..71060)	147				No SD element
121	-(71130..71339)	69				
122	-(71336..71560)	74	26989746 <i>Pseudomonas putida</i>	17313260 <i>Pseudomonas aeruginosa</i> phage phiCTX	Conserved hypothetical protein	
123	-(71557..71775)	72				
124	-(71887..72786)	299				
125	-(74731..75096)	121				
126	-(75189..75470)	93				
127	-(75656..75919)	87				Weak SD element
128	-(75944..76816)	290				